arXiv:nucl-th/0301011v1 6 Jan 2003

Vector Meson Photoproduction Processes Near Threshold

Yongseok Oh*
Institute of Physics and Applied Physics, Yonsei University, Seoul 120-749, Korea

(Received February 8, 2008)

We discuss the photoproduction processes of light vector mesons (ρ, ω, and ϕ) from the nucleon near threshold. We first develop a simple model based on meson exchanges which is modified by the nucleon pole terms. We then extend this model to study other physically interesting topics. As examples, we discuss the missing nucleon resonances problem in ω photoproduction and the direct ϕNN coupling constant in ϕ photoproduction. The calculated cross sections are compared with the recent experimental data. Various spin observables are discussed, which may be measured at current photon/electron facilities such as TJNAF and SPring-8 of RCNP. Precise measurements of such quantities would provide very useful information to understand the production mechanism.

PACS numbers: 13.60.Le, 13.25.Gv, 14.20.Gk, 24.70.+s, 25.20.Lj
Keywords: vector meson photoproduction, polarization asymmetries, nucleon resonances, OZI violation

I. INTRODUCTION

At high energies and low momentum transfers, the exclusive electromagnetic production of vector mesons has been explained successfully by the (soft) Pomeron exchange model [1–3]. (For the failure of the soft Pomeron model at large t, see, for example, Refs. [4–6].) However, at low energies near threshold, it is well known that the meson exchange mechanisms or the exchange of the secondary Regge trajectories become important or even dominant, of which examples are the π exchange in ω production and the σ exchange in ρ production [7]. Furthermore, the nucleon exchange in s- and u-channels is known to be important in the large momentum transfer region at low energy, although its contribution becomes suppressed rapidly as the total energy increases.

The process of vector meson photoproduction, such as ρ, ω, and ϕ, attracts recent interests both theoretically and experimentally. This is because the vector meson production processes can give a very useful or unique probe to investigate several hadron physics problems. For example, the study of vector meson photoproduction is expected to be useful to resolve the so-called "missing resonances" problem [8, 9]. The constituent quark models predict a much richer nucleon excitation spectrum than what has been observed so far in the pion-nucleon channel [10, 11]. This has been attributed to the possibility that a lot of the predicted nucleon resonances (N^*) could couple weakly to the πN channel. Therefore it is necessary to search for the nucleon excitations in other reactions to resolve the missing resonances problem. Electromagnetic production of vector mesons is one of such reactions and is being investigated actively with kaon photoproduction [12]. Experimentally, data of vector meson photoproduction in the resonance region are now being rapidly accumulated at ELSA-SAPHIR of Bonn [13], Thomas Jefferson National Accelerator Facility (TJNAF) [14, 15], GRAAL of Grenoble [16], LEPS of SPring-8 [17], and etc. Theoretically, there are some recent progress [18–20] in this direction. In this paper, we discuss the role of the nucleon resonances in ω photoproduction in the resonance region.

Another interesting topic which will be discussed here is the direct coupling of the ϕ meson to the nucleon. The electromagnetic production of the ϕ from the nucleon has been suggested as a probe to study the hidden strangeness of the nucleon [21–25]. This is because the ϕ is nearly pure $s\bar{s}$ state so that its direct coupling to the nucleon is suppressed by the OZI rule. However, if there exists a non-vanishing $s\bar{s}$ sea quark component in the nucleon, the strange sea quarks can contribute to the ϕ production via the OZI evasion processes. Investigation of such processes can then be expected to shed light on the strangeness content of the nucleon, if any [26]. In this work, we investigate the direct ϕNN coupling with polarization observables in ϕ photoproduction.

This paper is organized as follows. In Sec. II, we develop models for vector meson photoproduction based on the Pomeron exchange, one-meson exchanges, and the nucleon exchange in s- and u-channels. By extending this simple model, in Sec. III, we study the nucleon resonances in ω photoproduction. Section IV is devoted to the direct ϕNN coupling study in ϕ photoproduction. Section V contains summary and discussion.

II. MODELS FOR VECTOR MESON PHOTOPRODUCTION

In this Section, we briefly discuss a simple model for vector meson photoproduction [27]. In order to confront the forthcoming data to extract the nucleon resonance parameters, it is crucial to understand the non-resonant (background) production processes which could interfere strongly with the resonant production amplitudes. As a step in this direction, we have investigated the ρ, ω, and ϕ photoproductions at low energies based on a model consisting of three mechanisms as shown in Fig. 1: Pomeron

---

[*] Electronic address: `yoh@phya.yonsei.ac.kr`

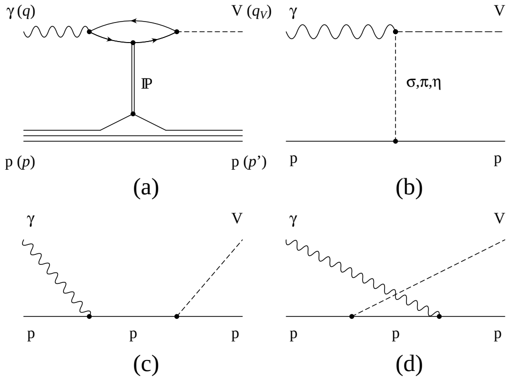

FIG. 1: Three mechanisms for vector meson ($V = \rho, \omega, \phi$) photoproduction: (a) Pomeron, (b) one-meson exchange, (c) and (d) s- and u-channel intermediate nucleon diagrams.

exchange, one-meson (π, η, σ) exchange, and the mechanism involving an intermediate nucleon in s- and u-channel (called nucleon exchange from now on).

A. Pomeron exchange

We first consider the Pomeron exchange depicted in Fig. 1(a). In this process, the incoming photon first converts into a $q\bar{q}$ pair, which interacts with the nucleon by the Pomeron exchange before forming the outgoing vector meson. The quark-Pomeron vertex is obtained by the Pomeron-photon analogy [1], which treats the Pomeron as a $C = +1$ isoscalar photon, as suggested by a study of nonperturbative two-gluon exchanges [28]. We then have

$$\begin{aligned} T^P_{fi} &= i12\sqrt{4\pi\alpha_{\rm em}}\beta_u G_P(s,t) F_1(t) \frac{m_V^2 \beta_f}{f_V} \\ &\times \frac{1}{m_V^2 - t}\left(\frac{2\mu_0^2}{2\mu_0^2 + m_V^2 - t}\right)\varepsilon^*_\mu(V)\varepsilon_\nu(\gamma) \\ &\times \bar{u}_{m'}(p')\{\not{q}\, g^{\mu\nu} - q^\mu\gamma^\nu\}u_m(p), \end{aligned} \tag{1}$$

where $\alpha_{\rm em} = e^2/4\pi$, m and m' are the spin projections of the initial and final nucleons, respectively [1–3, 24]. Here we denote the four-momenta of the initial nucleon, final nucleon, incoming photon, and outgoing vector meson by p, p', q, and q_V, respectively. $\varepsilon_\mu(V)$ and $\varepsilon_\nu(\gamma)$ are the polarization vectors of the vector meson and the photon, respectively. The Mandelstam variables are $s = W^2 = (p+q)^2$, $t = (p-p')^2$, $u = (p-q_V)^2$. The vector meson mass is represented by and m_V and F_1 is the isoscalar electromagnetic form factor of the nucleon. The Pomeron-exchange is described by the Regge form:

$$G_P(s,t) = \left(\frac{s}{s_0}\right)^{\alpha_P(t)-1} \exp\left\{-\frac{i\pi}{2}[\alpha_P(t)-1]\right\}. \tag{2}$$

The Pomeron trajectory is taken to be the usual form $\alpha_P(t) = 1.08 + \alpha'_P t$ with $\alpha'_P = 1/s_0 = 0.25$ GeV^{-2}. In Eq. (2), f_V is the vector meson decay constant. The parameters are chosen to reproduce the total cross section data at high energies $E_\gamma \geq 10$ GeV where the total cross section of vector meson photoproductions are completely dominated by the Pomeron-exchange.

B. Meson and nucleon exchanges

For the one-meson exchange (t-channel) diagram of Fig. 1(b), we consider scalar and pseudoscalar meson exchanges. The vector meson exchange is not allowed in this process and the possible exchange of axial vector mesons [5] is suppressed at low energies mainly because of their heavy masses and small coupling constants. We also include the nucleon exchanges in s- and u-channel as in Fig. 1(c,d). Those production amplitudes can be calculated from the following effective Lagrangian:

$$\mathcal{L} = \mathcal{L}_{V\gamma\varphi} + \mathcal{L}_{\varphi NN} + \mathcal{L}_\sigma + \mathcal{L}_{\gamma NN} + \mathcal{L}_{VNN}, \tag{3}$$

where

$$\mathcal{L}_{V\gamma\varphi} = \frac{eg_{V\gamma\varphi}}{2M_V}\varepsilon^{\mu\nu\alpha\beta}\partial_\mu V_\nu \partial_\alpha A_\beta \varphi, \tag{4}$$

where $\varphi = (\pi, \eta)$ and

$$\begin{aligned} \mathcal{L}_{\varphi NN} &= \frac{g_{\pi NN}}{2M_N}\bar{\psi}\gamma^\mu\gamma_5\partial_\mu\pi\psi + \frac{g_{\eta NN}}{2M_N}\bar{\psi}\gamma^\mu\gamma_5\psi\partial_\mu\eta, \\ \mathcal{L}_\sigma &= g_{\sigma NN}\bar{\psi}\sigma\psi \\ &\quad + \frac{eg_{\rho\gamma\sigma}}{2M_\rho}\,\mathrm{Tr}\,[\tau^3\partial_\mu\rho_\nu\,(\partial^\mu A^\nu - \partial^\nu A^\mu)\,\sigma], \\ \mathcal{L}_{\gamma NN} &= -e\bar{\psi}\left(\gamma_\mu\frac{1+\tau_3}{2}A^\mu - \frac{\kappa_N}{2M_N}\sigma^{\mu\nu}\partial_\nu A_\mu\right)\psi, \\ \mathcal{L}_{VNN} &= -\frac{g_{\rho NN}}{2}\bar{\psi}\left(\gamma_\mu\rho^\mu - \frac{\kappa_\rho}{2M_N}\sigma^{\mu\nu}\partial_\nu\rho_\mu\right)\psi \\ &\quad - g_{\omega NN}\bar{\psi}\left(\gamma_\mu\omega^\mu - \frac{\kappa_\omega}{2M_N}\sigma^{\mu\nu}\partial_\nu\omega_\mu\right)\psi, \end{aligned} \tag{5}$$

with the photon field A_μ, where π, η, ρ_μ ($= \boldsymbol{\tau}\cdot\boldsymbol{\rho}_\mu$), and ω_μ are the π^0, eta, rho, and omega meson fields, respectively.

The coupling constants $g_{V\gamma\pi}$ and $g_{V\gamma\eta}$ are obtained from the experimental partial widths [29] of the vector meson radiative decays $V \to \gamma\varphi$. We use $g^2_{\pi NN}/4\pi = 14.0$ and the SU(3) relation to obtain $g_{\eta NN}/g_{\pi NN} \simeq 0.35$. To account for the effects due to the finite hadron size at each vertex, the resulting Feynman amplitudes are regularized by the following form factors,

$$F_{MNN} = \frac{\Lambda_M^2 - M_M^2}{\Lambda_M^2 - t}, \qquad F_{V\gamma M} = \frac{\Lambda_{V\gamma M}^2 - M_M^2}{\Lambda_{V\gamma M}^2 - t}, \tag{6}$$

where ($\Lambda_\pi = 0.7$, $\Lambda_{V\gamma\pi} = 0.77$) and ($\Lambda_\eta = 1.0$, $\Lambda_{V\gamma\eta} = 0.9$) in GeV unit [30].

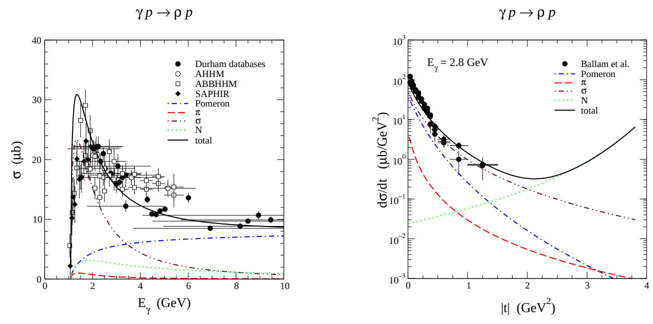

FIG. 2: (Left panel) Total cross section of ρ photoproduction. The experimental data are from Refs. [13, 34–36]. (Right panel) Differential cross sections of ρ photoproduction at $E_\gamma = 2.8$ GeV. The data are from Refs. [37, 38].

The scalar (σ) meson exchange was introduced to describe the ρ photoproduction [7].[1] This can be considered as an effective way to account for the two-π exchange in ρ production, which is expected to be significant because of the large branching ratio of $\rho \to \pi^+\pi^-\gamma$ decay. We use the parameters of Ref. [7] and $g_{V\gamma\sigma} \simeq 3.0$ to reproduce the total cross sections of ρ photoproduction near threshold. We do not consider the σ exchange in ω and ϕ photoproductions, since the radiative decays of these two vector mesons into $\pi^+\pi^-$ are much weaker. This could be understood by considering the current-field identity [7]. (See also Ref. [30].)

The nucleon exchange terms, Fig. 1(c,d), are obtained from the Lagrangian $\mathcal{L}_{\gamma NN}$ and $\mathcal{L}_{VNN}$, whose coupling constants are determined from the studies of πN scattering and pion photoproduction [32]. In this study, we do not consider the nucleon exchange in ϕ photoproduction by assuming $g_{\phi NN} \approx 0$ due to the OZI rule. This topic will be discussed in Sec. IV. The form factor F_V for VNN and γNN vertices is assumed to be of the form given by Ref. [33],

$$F_V(r) = \frac{\Lambda_{VNN}^4}{\Lambda_{VNN}^4 + (r - M_N^2)^2}, \tag{7}$$

where $r = (s, u)$ with $\Lambda_{VNN} \simeq 0.8$ GeV. The gauge invariance is restored by projecting out the gauge non-invariant part.

C. Results

With the production amplitudes given above, we have explored the extent to which the existing data of vector meson photoproductions can be described by the non-resonant (background) mechanisms.

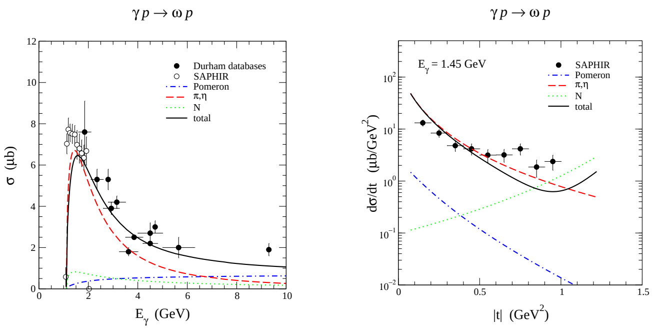

FIG. 3: Total and differential cross sections of ω photoproduction. The experimental data are from Refs. [13, 34, 37, 38].

The ρ photoproduction cross sections are calculated from the amplitudes due to Pomeron, π, σ exchanges and the nucleon exchange. In the left panel of Fig. 2 we show that the calculated total cross sections (solid curve) agree to a very large extent with the data up to $E_\gamma = 10$ GeV. The important role of the σ exchange (dot-dot-dashed curve) near threshold is also shown there. The dynamical content of the model can be better seen by investigating angular distributions. For example, given in the right panel of Fig. 2 is the angular distributions of the differential cross sections at $E_\gamma = 2.8$ GeV. We see that the contribution from the nucleon exchange (dotted curves) becomes dominant at large scattering angles. Therefore, precise measurements of the differential cross sections in the backward scattering region will shed light on the role of the intermediate nucleon states.

The ω photoproduction cross sections are calculated from the Pomeron, π and η exchanges, and the nucleon term. The predicted total and differential cross sections are compared with the data in Fig. 3. We see that the one-pion exchange (long dashed curves) dominates ω photoproduction up to $E_\gamma \approx 6$ GeV. The predicted total cross sections somewhat underestimate the recent SAPHIR data in the $E_\gamma \leq 2$ GeV region where the mechanisms involving the excitation of nucleon resonances are expected to play some roles. Similar to the case of ρ photoproduction, the nucleon-term dominates at large $|t|$.

For ϕ photoproduction, we consider the Pomeron and pseudoscalar meson (π and η) exchanges only. We refer the calculations on the scalar meson exchanges and direct ϕ radiation arising from the non-vanishing ϕNN coupling to Ref. [30] and the effects of non-vanishing strangeness of the nucleon to Refs. [22, 24]. In Fig. 4 we show that the predicted total and differential cross sections agree well with the very limited data. Contrary to the cases of ρ and ω photoproductions, the Pomeron exchange (dash-dotted curves) gives the major contribution to the *total* cross section even at energies near threshold. This is mainly due to the fact that the coupling of the ϕ to the nucleon is suppressed by the OZI rule. The contributions from π and η exchanges are also found to be small.

---

[1] One can describe the ρ photoproduction data by the exchange of f_2 trajectory instead of σ exchange [2, 31].

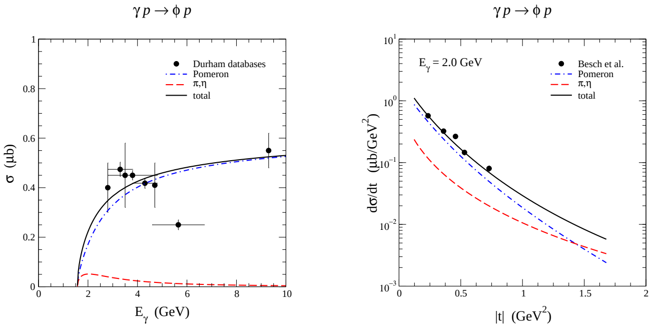

FIG. 4: Total and differential cross sections of ϕ photoproduction. The experimental data are from Refs. [34, 39].

III. NUCLEON RESONANCES IN ω PHOTOPRODUCTION

The role of the nucleon excitations in vector meson photoproduction was studied recently by Zhao *et al.* [18, 40] using an effective Lagrangian method within the SU(6) × O(3) constituent quark model. In this work, we are motivated by the predictions by Capstick and Roberts [41, 42]. They started with a constituent quark model which accounts for the configuration mixing due to the residual quark-quark interactions [43]. The predicted baryon wave functions are considerably different from those of the $\mathrm{SU}(6)\times\mathrm{O}(3)$ model employed by Zhao *et al.* in Refs. [18, 40]. The second feature of the predictions from Refs. [41, 42] is that the meson decays are calculated from the correlated wave functions by using the ${}^3P_0$ model. Thus it would be interesting to see how these predictions differ from those of Refs. [18, 40] and can be tested against the data of vector meson photoproduction. We will focus on ω photoproduction in this work, simply because its non-resonant reaction mechanisms are much better understood.

In order to estimate the nucleon resonance contributions we make use of the quark model predictions on the resonance photo-excitation $\gamma N \to N^*$ and the resonance decay $N^* \to \omega N$ reported in Refs. [41, 42] using a relativised quark model. We calculate the s-channel diagrams only since the crossed, u-channel, N^* amplitude cannot be calculated from the informations available in Refs. [41, 42]. In this study, we consider 12 positive parity and 10 negative parity nucleon resonances up to spin-9/2. Most of them are "missing" so far. The resonance parameters taken from Refs. [41, 42] can be found in Ref. [20] with the other cutoff parameters. Here we should also mention that we can not account for the resonances with its predicted masses less than the ωN threshold, since their decay vertex functions with an off-shell momentum are not available. (See Ref. [44] for the contributions from the N^*'s below the threshold.)

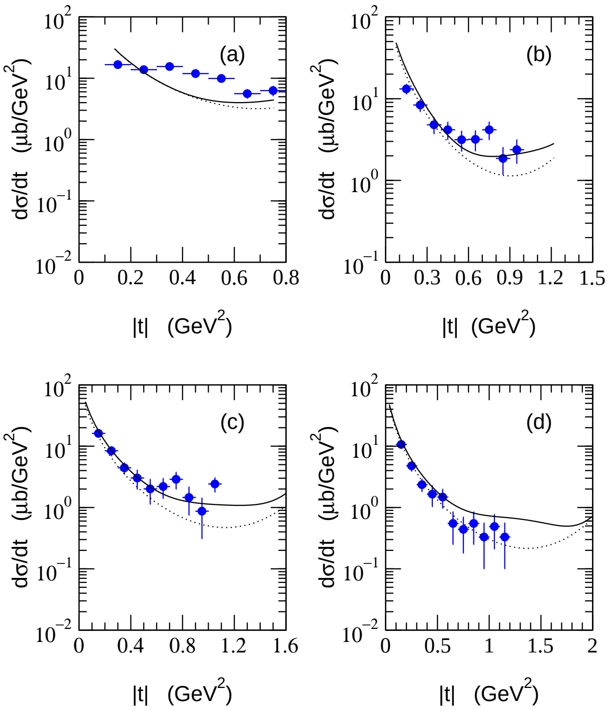

FIG. 5: Differential cross sections for the $\gamma p \to p\omega$ reaction as a function of $|t|$ at different energies: $E_\gamma =$ (a) 1.23, (b) 1.45, (c) 1.68, and (d) 1.92 GeV. The solid and dotted curves are calculated respectively with and without including N^* effects. Data are taken from Ref. [13].

The total resonance effects are shown in Fig. 5. The solid curves are from our full calculations, while the dotted curves are from the calculations without including N^* excitations. The results shown in Fig. 5 indicate that it is rather difficult to test our predictions by considering only the angular distributions, since the N^*'s influence is mainly in the large scattering angle region where accurate measurements are perhaps still difficult. On the other hand, the forward cross sections seem to be dominated by the well-understood pseudoscalar-meson exchange and Pomeron exchange. Therefore, one can use this well-controlled background to examine the N^* contributions by exploiting the interference effects in the spin observables. We also found that the contributions from $N\frac{3}{2}^+(1910)$ and $N\frac{3}{2}^-(1960)$ are the largest at all energies considered in Fig. 5.

To further facilitate the experimental tests of our predictions, we have investigated spin observables. We have identified two polarization observables which are sensitive to the N^* contributions at forward angles, where precise measurements might be more favorable because the cross sections are peaked at small $|t|$. Shown in Fig. 6 are the parity asymmetry P_σ and the beam-target double asymmetry C_{zz}^{BT} at $\theta = 0$, where θ is the scattering angle in the center of mass frame. One can find the sensitivity of those asymmetries on the nucleon resonances. Therefore experimental test of our predictions will be a useful step toward resolving the so-called "missing resonance problem" or distinguishing various QCD-inspired models for hadron.

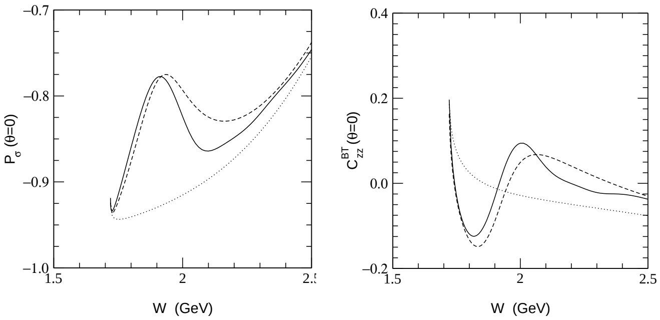

FIG. 6: Parity asymmetry P_σ at $\theta = 0$ as a function of W. The dotted curves are calculated without including N^* effects, the dashed curves include contributions of $N\frac{3}{2}^+(1910)$ and $N\frac{3}{2}^-(1960)$ only, and the solid curves are calculated with all N^*'s considered in this calculation.

IV. $g_{\phi NN}$ IN ϕ PHOTOPRODUCTION

If we assume the ideal mixing of the ϕ with the ω, the direct coupling of the nucleon and the ϕ should be suppressed by the OZI rule. In nature, the deviation from the ideal mixing is very small and the direct ϕNN coupling should be very small, although not vanish. In this Section, we discuss the effective ϕNN coupling in ϕ photoproduction. For this purpose, we use the effective Lagrangian for the ϕNN interaction as in Eq. (5).

Even if we assume the ideal mixing between the ϕ and the ω, non-vanishing effective ϕNN coupling is allowed by the kaon loops and hyperon excitations. The estimated ϕNN coupling is very small, $g_{\phi NN} \simeq -0.24$ [45], which is consistent with the OZI rule prediction. However the analyses on the electromagnetic nucleon form factors [46–48] and the baryon-baryon scattering [49] favor a large ϕNN vector coupling constant which strongly violates the OZI rule: $g_{\phi NN}/g_{\omega NN} = -0.3 \sim -0.43$, therefore $g_{\phi NN} = -2.3 \sim -4.7$ with $g_{\omega NN} = 7.0 \sim 11.0$ [32]. In our study the nucleon pole terms are responsible to the ϕ photoproduction at large $|t|$ and we find that $|g_{\phi NN}| = 3.0$ can reproduce the recent CLAS data [50], which is consistent with the Regge trajectory study of Ref. [51].

In Fig. 7, we compare our predictions with the recent CLAS data [14] by assuming $g_{\phi NN} = -3.0$. The role of the tensor coupling is found to be negligible if $\kappa_\phi < 1$. We also found that vector meson density matrix and some asymmetries are sensitive to the phase of the ϕNN coupling constant. As an example, we present our prediction of the parity asymmetry P_σ and the photon polarization asymmetry Σ_ϕ in Fig. 8. The details can be found in Ref. [50].

V. SUMMARY AND DISCUSSION

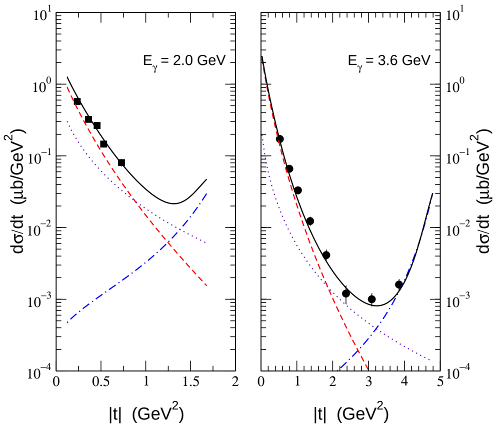

FIG. 7: Differential cross sections of ϕ photoproduction at $E_\gamma = 2.0$ GeV and 3.6 GeV. The results are from Pomeron exchange (dashed), pseudoscalar-meson exchange (dotted), nucleon pole terms with $g_{\phi NN} = -3.0$ (dot-dashed), and the full amplitude (solid). The experimental data are from Ref. [39] (filled squares) and Ref. [14] (filled circles).

In this paper, we briefly review models to understand the production mechanism of vector meson photoproduction near threshold. We first discuss models based on the Pomeron, meson, and nucleon exchanges. With those background amplitudes, the role of nucleon resonances is studied in ω photoproduction and we found that measuring polarization asymmetries is very useful to identify the contributions from the nucleon resonances. The effective ϕNN coupling is also discussed within ϕ photoproduction. The results show that the recent CLAS experiment could be understand by a fairly large ϕNN coupling constant. Other physical quantities are suggested to confirm and test the model predictions.

Finally we have to mention that the extraction of N^* parameters from experimental data depends strongly on the accuracy of the nonresonant amplitudes. Therefore,

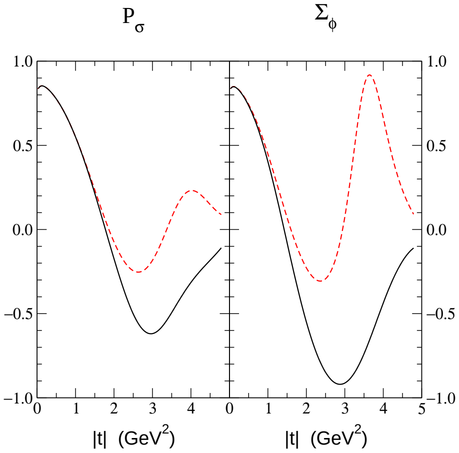

FIG. 8: Parity asymmetry P_σ and the photon polarization asymmetry Σ_ϕ in ϕ photoproduction at $E_\gamma = 3.6$ GeV with the full amplitude. The solid lines are with $g_{\phi NN} = -3.0$ and the dashed lines with $g_{\phi NN} = +3.0$.

it is legitimate to develop a dynamical model for the coupled-channel effects, which should satisfy the unitarity condition [52, 53]. The importance of the final state interaction to extract the direct ϕNN coupling should also be studied. Together with those theoretical studies, it is very crucial to test the models by experiments. Therefore, experimental research at, for example, TJNAF and SPring-8 would be very important to understand the production mechanisms of the electromagnetic production of vector mesons and the hadron structure.

I have benefited from discussions and collaboration with H. Bhang, N. I. Kochelev, T.-S. H. Lee, D.-P. Min, T. Morii, A. I. Titov, and S. N. Yang. I am also grateful to V. D. Burkert, M. Fujiwara, Hungchong Kim, Su Houng Lee, T. Nakano, E. Smith, and V. Vento for fruitful discussions. This work was supported by the Brain Korea 21 project of Korean Ministry of Education and the International Collaboration Program of KOSEF under Grant No. 20006-111-01-2.

[1] A. Donnachie and P. V. Landshoff, Nucl. Phys. B **244**, 322 (1984).
[2] J.-M. Laget and R. Mendez-Galain, Nucl. Phys. A **581**, 397 (1995).
[3] M. A. Pichowsky and T.-S. H. Lee, Phys. Rev. D **56**, 1644 (1997).
[4] A. Donnachie and P. V. Landshoff, Phys. Lett. B **437**, 408 (1998); **478**, 146 (2000).
[5] N. I. Kochelev, D.-P. Min, Y. Oh, V. Vento, and A. V. Vinnikov, Phys. Rev. D **61**, 094008 (2000); Nucl. Phys. B (Proc. Suppl.) **99**, 24 (2001).
[6] Y. Oh, N. I. Kochelev, D.-P. Min, V. Vento, and A. V. Vinnikov, Phys. Rev. D **62**, 017504 (2000).
[7] B. Friman and M. Soyeur, Nucl. Phys. A **600**, 477 (1996).
[8] S. Capstick and W. Roberts, Prog. Part. Nucl. Phys. **45**, S241 (2000).
[9] V. D. Burkert, hep-ph/0207149; hep-ph/0210321.
[10] N. Isgur and G. Karl, Phys. Lett. **72B**, 109 (1977); Phys. Rev. D **18**, 4187 (1978); **19**, 2653 (1979), **23**, 817(E) (1981).
[11] R. Koniuk and N. Isgur, Phys. Rev. D **21**, 1868 (1980).
[12] T. Mart and C. Bennhold, Phys. Rev. C **61**, 012201 (1999); J. K. Ahn, in these proceedings.
[13] F. J. Klein, Ph.D. thesis, Bonn Univ. (1996); πN Newslett. **14**, 141 (1998).
[14] CLAS Collaboration, E. Anciant *et al.*, Phys. Rev. Lett. **85**, 4682 (2000).
[15] CLAS Collaboration, K. Lukashin *et al.*, Phys. Rev. C **63**, 065205 (2001); M. Battaglieri *et al.*, Phys. Rev. Lett. **87**, 172002 (2001); M. Battaglieri *et al.*, hep-ex/0210023.
[16] J. Ajaka *et al.*, Talk at SPIN 2000, AIP Conf. Proc. No. **570** (2001) p. 198.
[17] T. Nakano, Talk at SPIN 2000, AIP Conf. Proc. No. **570** (2001) p. 189; in these proceedings.
[18] Q. Zhao, Z. Li, and C. Bennhold, Phys. Lett. B **436**, 42 (1998). Phys. Rev. C **58**, 2393 (1998).
[19] Q. Zhao, Phys. Rev. C **63**, 025203 (2001).
[20] Y. Oh, A. I. Titov, and T.-S. H. Lee, Phys. Rev. C **63**, 025201 (2001).
[21] E. M. Henley, G. Krein, S. J. Pollock, and A. G. Williams, Phys. Lett. B **269**, 31 (1991); E. M. Henley, G. Krein, and A. G. Williams, *ibid.* **281**, 178 (1992).
[22] A. I. Titov, Y. Oh, and S. N. Yang, Chin. J. Phys. (Taipei) **32**, 1351 (1994); Phys. Rev. Lett. **79**, 1634 (1997).
[23] A. I. Titov, S. N. Yang, and Y. Oh, Nucl. Phys. A **618**, 259 (1997).
[24] A. I. Titov, Y. Oh, S. N. Yang, and T. Morii, Phys. Rev. C **58**, 2429 (1998).
[25] Y. Oh, A. I. Titov, S. N. Yang, and T. Morii, Phys. Lett. B **462**, 23 (1999); Nucl. Phys. A **684**, 354 (2001).
[26] J. Ellis, M. Karliner, D. E. Kharzeev, and M. G. Sapozhnikov, Nucl. Phys. A **673**, 256 (2000); J. Ellis, Nucl. Phys. A **684**, 53 (2001).
[27] Y. Oh, A. I. Titov, and T.-S. H. Lee, Talk at NSTAR 2000 Workshop, nucl-th/0004055.
[28] P. V. Landshoff and O. Nachtmann, Z. Phys. C **35**, 405 (1987).
[29] Particle Data Group, C. Caso *et al.*, Eur. Phys. J. C **3**, 1 (1998).
[30] A. I. Titov, T.-S. H. Lee, H. Toki, and O. Streltsova, Phys. Rev. C **60**, 035205 (1999).
[31] A. Donnachie and P. V. Landshoff, Phys. Lett. B **296**, 227 (1992).
[32] T. Sato and T.-S. H. Lee, Phys. Rev. C **54**, 2660 (1996).
[33] B. C. Pearce and B. K. Jennings, Nucl. Phys. A **528**, 655 (1991).
[34] The Durham RAL Databases, http://durpdg.dur.ac.uk/HEPDATA/REAC.
[35] W. Struczinski *et al.*, Nucl. Phys. B **108**, 45 (1976).
[36] R. Erbe *et al.*, Phys. Rev. **175**, 1669 (1968).
[37] J. Ballam *et al.*, Phys. Rev. D **5**, 545 (1972).
[38] J. Ballam *et al.*, Phys. Rev. D **7**, 3150 (1973).
[39] H. J. Besch *et al.*, Nucl. Phys. B **70**, 257 (1974).
[40] Q. Zhao, J.-P. Didelez, M. Guidal, and B. Saghai, Nucl. Phys. A **660**, 323 (1999).
[41] S. Capstick, Phys. Rev. D **46**, 2864 (1992).
[42] S. Capstick and W. Roberts, Phys. Rev. D **49**, 4570 (1994).
[43] S. Godfrey and N. Isgur, Phys. Rev. D **32**, 189 (1985); S. Capstick and N. Isgur, *ibid.* **34**, 2809 (1986).
[44] A. I. Titov and T.-S. H. Lee, Phys. Rev. C **66**, 015204 (2002).
[45] U.-G. Meißner, V. Mull, J. Speth, and J. W. Van Orden, Phys. Lett. B **408**, 381 (1997).
[46] H. Genz and G. Höhler, Phys. Lett. **61B**, 389 (1976).
[47] G. Höhler *et al.*, Nucl. Phys. B **114**, 505 (1976).
[48] R. L. Jaffe, Phys. Lett. B **229**, 275 (1989).
[49] M. M. Nagels, T. A. Rijken, and J. J. de Swart, Phys. Rev. D **12**, 744 (1975); **15**, 2547 (1977); **20**, 1633 (1979).
[50] Y. Oh and H. C. Bhang, Phys. Rev. C **64**, 055207 (2001).
[51] J. M. Laget, Phys. Lett. B **489**, 313 (2000).
[52] Y. Oh and T.-S. H. Lee, Phys. Rev. C **66**, 045201 (2002); Talk at PANIC 2002 (2002), nucl-th/0211054.
[53] G. Penner and U. Mosel, nucl-th/0207069.